Electroweak measurements from W and Z/γ^* properties with the ATLAS detector

M. Bellomo (CERN)
on behalf of the ATLAS Collaboration

17-24 July, 2013

2013 European Physical Society Conference on High Energy Physics

The ATLAS Detector

- ⋆ EM calorimeter and tracking up to $|\eta| < 2.5 \Rightarrow$ **electrons**
- ⋆ Muon spectrometer up to $|\eta| < 2.7$, trigger coverage to $|\eta| < 2.4 \Rightarrow$ **muons**
- ⋆ Calorimetric coverage up to $|\eta| < 4.9 \Rightarrow$ jets, $E_{\mathrm{T}}^{\mathrm{miss}}$, **forward electrons**

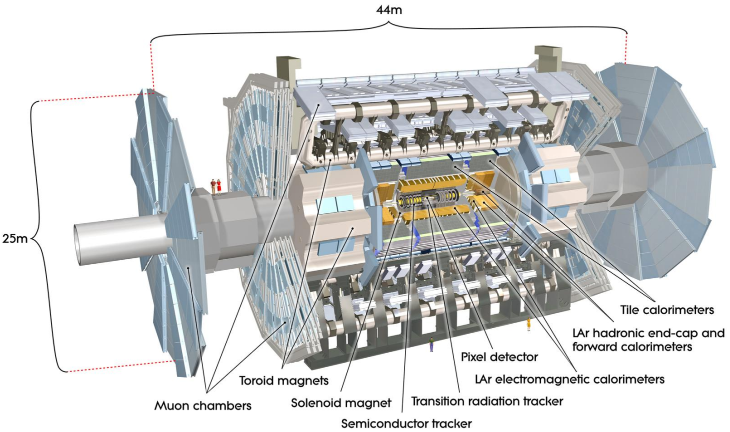

W and Z production at LHC

Drell-Yan production of W and Z bosons calculable to high orders in pQCD

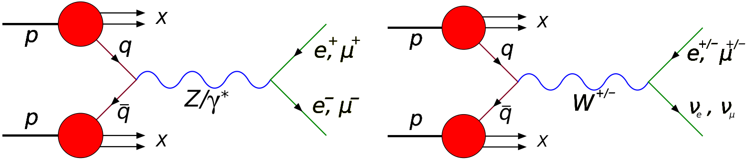

- ⋆ Integrated and rapidity-dependent cross-sections
  - ✓ Testing ground for Parton Distribution Functions (PDFs)
- ⋆ Boson p_T and ϕ^* measurements
  - ✓ Test of resummation and perturbative QCD (pQCD)
- ⋆ High mass Drell-Yan cross-section
  - ✓ Tests of pQCD, EW corrections, γ-induced processes, sensitive to poorly known $\bar{q}$ PDF at large-x
- ⋆ Forward-backward Z asymmetry measurement
  - ✓ Measurement of $sin^2\theta_W^{eff}$
- ⋆ Angular distributions in $W \to \ell\nu$ decays
  - ✓ Measurements of W and τ polarizations

W, Z inclusive cross-sections

Phys. Rev. D85 (2012) 072004, Phys.Rev.Lett. 109 (2012) 012001

HERA and ATLAS W,Z data is fit with the HERAFITTER framework

($Q_0^2 = 1.9\ GeV^2$, $m_c = 1.4\ GeV$, $m_b = 4.75\ GeV$, $\alpha_s(M_Z) = 0.1176$)

- ⋆ Fits are run with fixed $\bar{s}/\bar{d} = 0.5$ and leaving $\bar{s}(x)$ free (with $s = \bar{s}$)
- ⋆ The "free $\bar{s}$ fit" leads to better χ^2 to ATLAS data and determines $r_s = 0.5(s+\bar{s})/\bar{d} = 1.00^{+0.25}_{-0.28}$

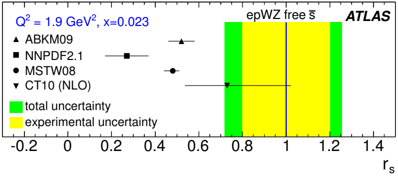

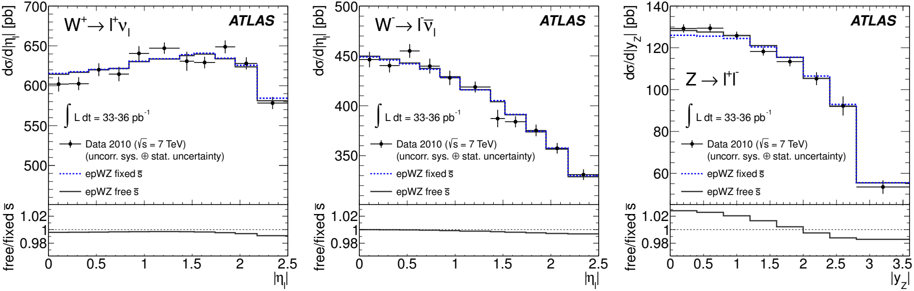

↪ More on PDFs from V. Radescu's talk in QCD session

W and Z p_T measurements

Phys.Rev. D85 (2012) 012005, Phys.Lett. B705 (2011) 415-434

- ★ Boson p_T in $Z \to \ell\ell$ decays
- ★ Precision still statistically limited
- ★ Systematic uncertainty in 2 – 5% range

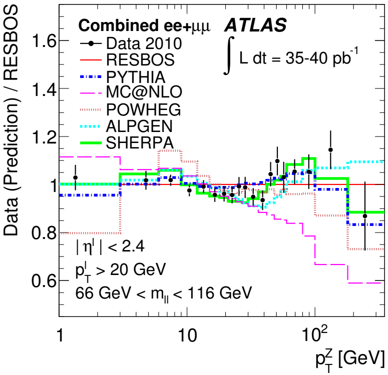

- ★ Boson p_T in $W \to \ell\nu$ decays
- ★ Uncertainty dominated by systematics, in the range 2 – 5% for $p_T < 100\,GeV$

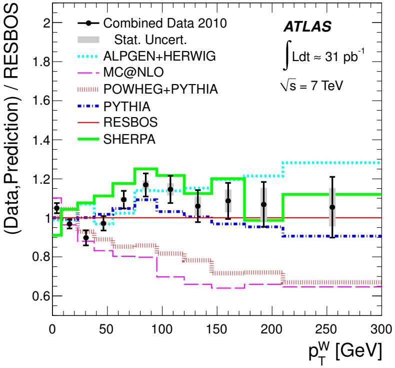

Looking for an improvement especially in the low-p_T region ($p_T < m_Z$) ...
(important to test resummation calculations, eg. Higgs momentum predictions)

$Z \to \ell\ell$ cross-section vs. ϕ^*

Phys. Lett. B 720 (2013) 32-51

- ⋆ Measurement of an angular observable $\propto p_T^Z / m_{\ell\ell}$

  $\phi^* \equiv tan(\phi_{acop}/2) \cdot sin(\theta^*_\eta)$

  - ✓ Depends only on tracks direction ⇒ smaller sensitivity to experimental syst.
  - ✓ Probes the same physics as p_T^Z ⇒ ϕ^* in (0,1) probes p_T^Z up to 100 GeV

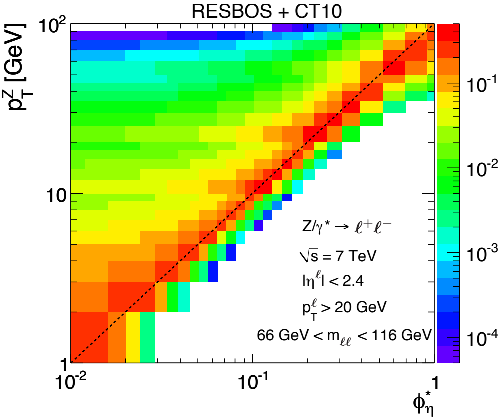

$Z \rightarrow \ell\ell$ cross-section vs. ϕ^*

Phys. Lett. B 720 (2013) 32-51

- ⋆ Measurement of an angular observable $\propto p_T^Z/m_{\ell\ell}$
  $\phi^* \equiv tan(\phi_{acop}/2) \cdot sin(\theta^*_\eta)$
- ⋆ Measurements done in electron and muon channels
- ⋆ Cross-sections are measured for $p_T^\ell > 20\ GeV$, $|\eta_\ell| < 2.4$ and $66 < m_{\ell\ell} < 116\ GeV$
- ⋆ Multi-jet background derived from data fitting the Z lineshape
- ⋆ Total background very small, ~ 0.6%
  ⇒ high-precision measurement

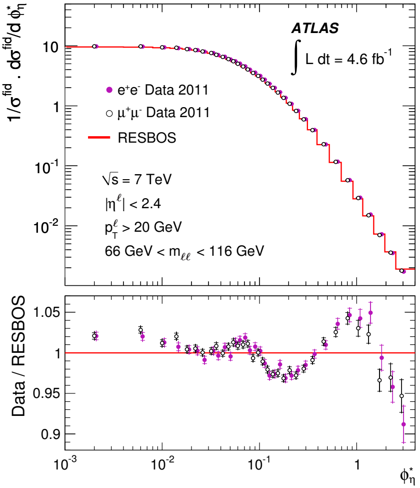

- ⋆ Systematics at 0.1 – 0.3% level, smaller than statistical uncertainty (0.3%)
  - ✓ Backgrounds, angular resolution, unfolding, MC statistical uncertainty, QED FSR uncertainty ... all effects at ~ 0.1 level

$Z \to \ell\ell$ cross-section vs. ϕ^*

Phys. Lett. B 720 (2013) 32-51

- ⋆ Comparison to MC predictions and NNLL calculations

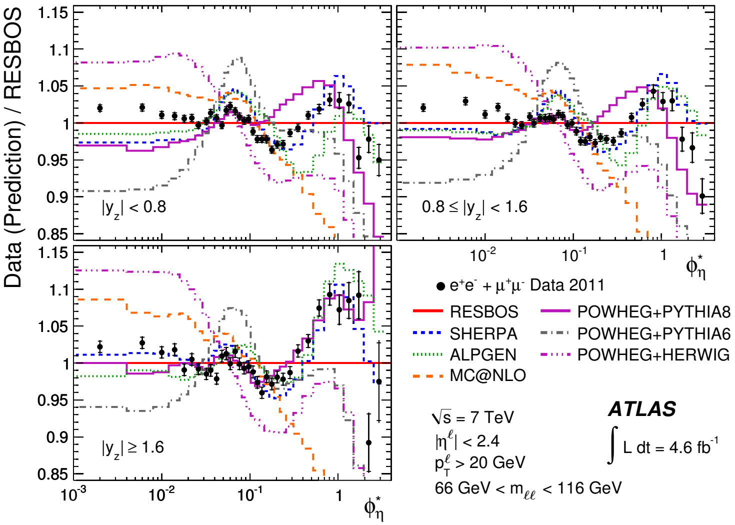

High mass Drell-Yan cross-sections

arXiv:1305.4192

- ⋆ Cross-sections are measured for $p_T^\ell > 25\ GeV$, $|\eta_\ell| < 2.5$ and $116 < m_{\ell\ell} < 1500\ GeV$
- ⋆ Main backgrounds from dijet and W+jets (6-16%), derived from data measuring the jet-to-electron fake rate in jet-enriched control sample

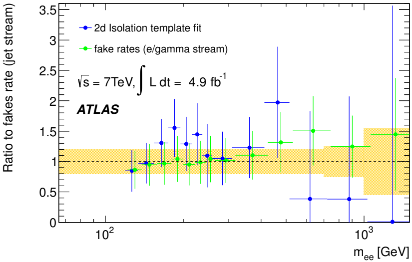

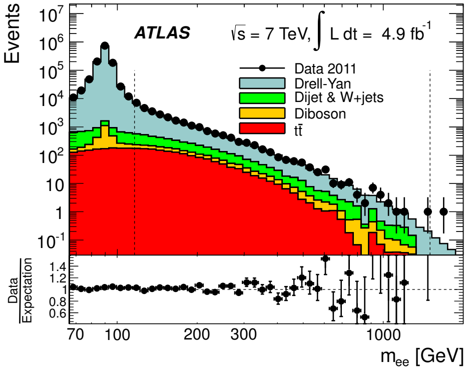

- ⋆ $Z \rightarrow ee$ spectrum measured in data compared to prediction from PYTHIA w/ NNLO QCD and NLO EW k-factors (plus backgrounds)

High mass Drell-Yan cross-sections

arXiv:1305.4192

- ⋆ Systematic uncertainty (4.2 – 9.8%) dominated by electron calibration and efficiencies, statistically dominated for $m_{ee} > 400\ GeV$

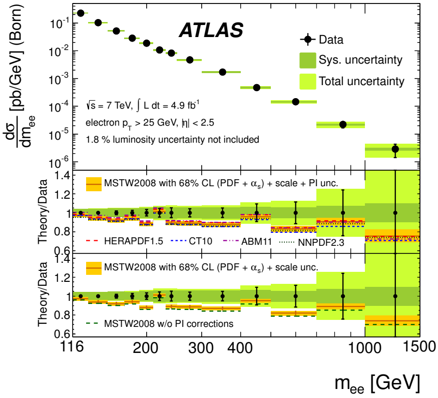

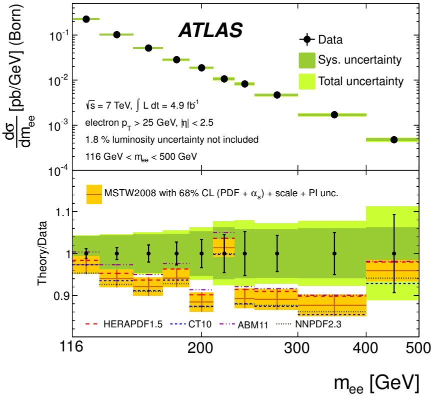

- ⋆ Data compared to NNLO QCD FEWZ calculations, including NLO EW corrections, and with different NNLO PDFs
  - ✓ γ-induced contribution (1 – 8%) and real W, Z FSR (0.1 – 2%) also included

Forward-backward Z asymmetry measurement

ATLAS-CONF-2013-043

- ⋆ Measurement of A_{FB} in $Z \to \ell\ell$ decays $\Rightarrow$ extraction of $sin^2\theta_W^{eff}$
- ⋆ Electrons selected with $E_T > 25\,GeV$ in central ($|\eta| < 2.47$) and forward ($2.5 < |\eta| < 4.9$) regions
- ⋆ Muons from inner tracker and muon-spectrometer measurements selected with $p_T > 20\,GeV$ and $|\eta| < 2.4$

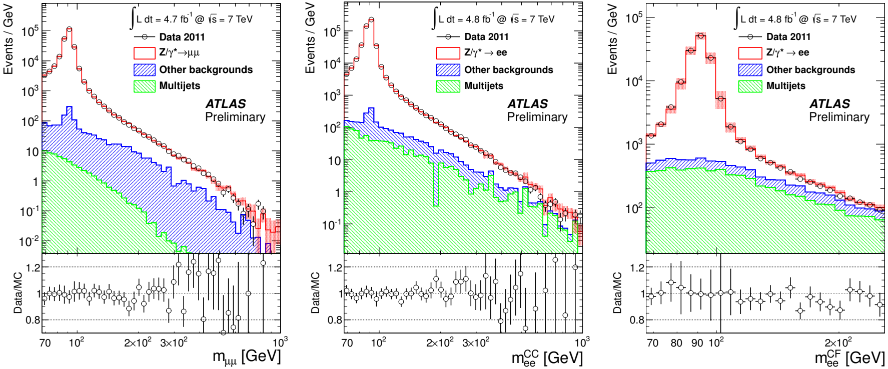

"CC" = two central electrons, "CF" = one central and one forward electron

Forward-backward Z asymmetry measurement

ATLAS-CONF-2013-043

- ★ Electrons selected with $E_T > 25\,GeV$ in central ($|\eta| < 2.47$) and forward ($2.5 < |\eta| < 4.9$) regions
  - ✓ "Forward" electrons important to reconstruct Z events at large rapidity where direction of incoming quark is better determined
  - ✓ A_{FB} is already visible from the reco-level distribution

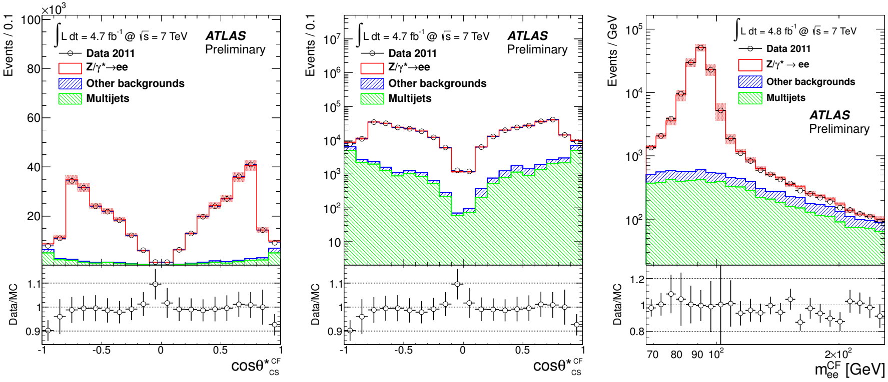

$cos\theta^*_{CS}$ for central-forward electrons in Collins-Soper frame

Forward-backward Z asymmetry measurement

ATLAS-CONF-2013-043

- ⋆ Bayesian unfolded A_{FB} spectrum compared to PYTHIA prediction including QED FSR and NLO QCD corrections
  - ✓ unfolding accounts for detector effects and QED corrections
- ⋆ Systematic uncertainties from unfolding (checked with a data re-weighting procedure), MC dependence and higher order QCD and EW corrections, PDFs, MC statistics, backgrounds and other experimental effects

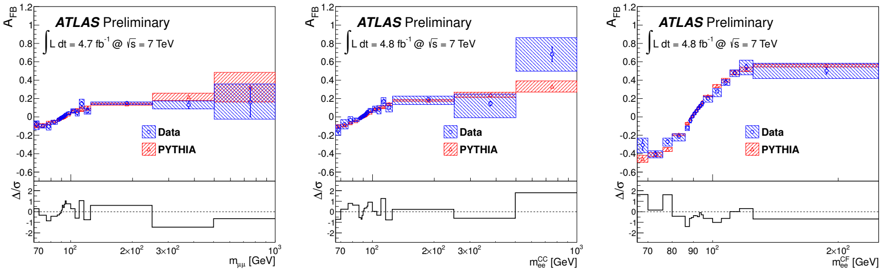

"CC" = two central electrons, "CF" = one central and one forward electron

Forward-backward Z asymmetry measurement

ATLAS-CONF-2013-043

$sin^2\theta_W^{eff}$ is measured from raw A_{FB} spectra fitting with MC templates obtained varying the input value of the weak mixing angle

$$sin^2\theta_W^{eff}\,(combined) = 0.2297 \pm 0.0004\,(stat) \pm 0.0009\,(syst)$$

- ⋆ Uncertainty dominated by PDFs, MC statistics and electron calibration are next

Uncertainty ($\times 10^{-4}$)	e_{CC}	e_{CF}	μ	com
PDF	9	5	9	7
MC stat	9	5	9	4
e energy scale	4	6	–	4
e energy resol	4	5	–	3
μ momen. scale	–	–	5	2
HO corrections	3	1	3	2
Other sources	1	1	2	2

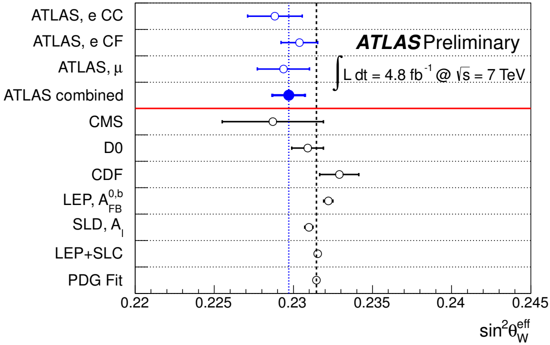

- ⋆ Precision comparable to D0 result from Tevatron
- ⋆ Measurement in agreement within 1.8σ with PDG global fit

W polarization at high p_T

Eur. Phys. J. C72 (2012) 2001

★ Helicity fractions, f_0 and $f_L - f_R$, measured from angular distribution in transverse plane: $cos\theta_{2D} = \vec{p}_T^{\ell *} \cdot \vec{p}_T^{W} \ / \ |\vec{p}_T^{\ell *}||\vec{p}_T^{W}|$

✓ Measurements done for $35 < p_T^W < 50\,GeV$ and $p_T^W > 50\,GeV$ regions

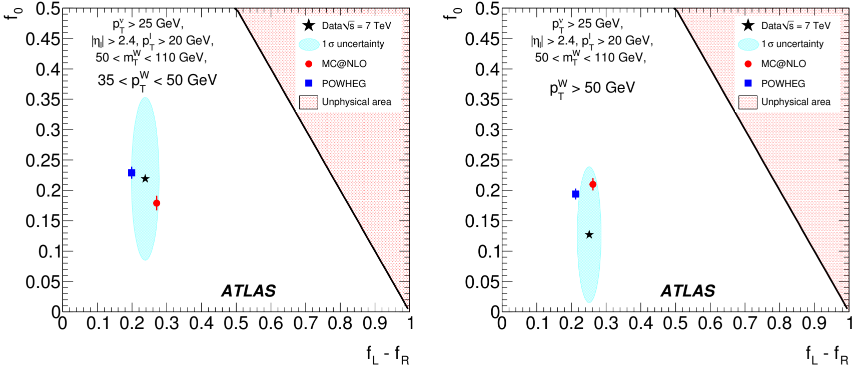

★ $f_L - f_R$ measured with 12–14% syst. uncertainty, dominated by hadronic recoil scale uncertainty (statistical uncertainty in 6–8% range)

★ Results compared to NLO QCD predictions from `MC@NLO`, `POWHEG` MCs

τ polarization in $W \to \tau\nu$ decays

Eur. Phys. J. C72 (2012) 2062

- First measurement at hadron collider and first probe of helicity structure of $W \to \tau\nu$ coupling at high Q^2
  - ✓ Done in hadronic τ decay channels with single charged hadron
- General method based on energy sharing of charged and neutral πs in τ decay relative to $p_T^{\tau,vis}$ ("charged asymmetry", Υ)
- Systematic uncertainty dominated by τ and cluster energy calibrations

Source	$+\Delta P_\tau$	$-\Delta P_\tau$
Energy scale central	0.042	0.063
Energy scale forward	0.007	0.002
E_T^{miss} resolution	0.014	-
No FCal	0.003	-
τ identification	0.005	0.006
Trigger	0.007	0.006
MC model	0.020	0.020
W cross-section	0.005	0.005
Z cross-section	0.006	0.006
Combined	0.05	0.07

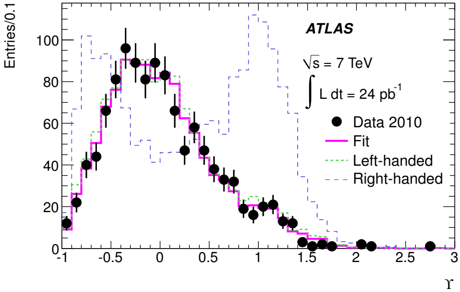

- Measured value in agreement with SM within uncertainties (5 – 7%)

$P_\tau = -1.06 \pm 0.04\,(stat)^{+0.05}_{-0.07}\,(syst)$ (Bayesian 95% credibility interval $[-1, -0.91]$)

Summary & Outlook

W,Z Physics at LHC can be measured with very high precision

- ⋆ Measurements of (pseudo-)rapidity spectra of $W \to \ell\nu$ and $Z \to \ell\ell$ decays can lead to new insights on PDFs, hint of unsuppressed strangeness in proton at low x from W,Z 2010 data fitted with HERA data
- ⋆ Very precise measurement of ϕ^* in $Z \to \ell\ell$ decay allows to make stringent tests of resummation calculations
- ⋆ The measurement of NC Drell-Yan cross-section up to 1.5 TeV allows to tests pQCD and EW corrections with sensitivity to γ-induced processes
- ⋆ First ATLAS measurement of $sin^2\theta_W^{eff}$ analyzing A_{FB} in $Z \to \ell\ell$ decays, already as precise as best Tevatron result
- ⋆ W polarization measured in $W \to \ell\nu$ decays at high transverse momentum allows to test QCD calculations for better understanding of the modeling of angular distributions
- ⋆ First measurement of τ polarization in $W \to \tau\nu$ decays at hadron colliders, proof of a general methodology applicable also to Z and H bosons

Summary & Outlook

W,Z Physics at LHC can be measured with very high precision

- ⋆ Measurements of (pseudo-)rapidity spectra of $W \rightarrow \ell\nu$ and $Z \rightarrow \ell\ell$ decays can lead to new insights on PDFs, hint of unsuppressed strangeness in proton at low x from W,Z 2010 data fitted with HERA data
- ⋆ Very precise measurement of ϕ^* in $Z \rightarrow \ell\ell$ decay allows to make stringent tests of resummation calculations
- ⋆ The measurement of NC Drell-Yan cross-section up to 1.5 TeV allows to tests pQCD and EW corrections with sensitivity to γ-induced processes
- ⋆ First ATLAS measurement of $sin^2\theta_W^{eff}$ analyzing A_{FB} in $Z \rightarrow \ell\ell$ decays, already as precise as best Tevatron result
- ⋆ W polarization measured in $W \rightarrow \ell\nu$ decays at high transverse momentum allows to test QCD calculations for better understanding of the modeling of angular distributions
- ⋆ First measurement of τ polarization in $W \rightarrow \tau\nu$ decays at hadron colliders, proof of a general methodology applicable also to Z and H bosons

More to come "soon" with 2011 dataset and then 8 TeV collisions ...

Back-up slides

LHC runs

- ⋆ LHC delivered $p-p$ collision data in three runs at 7 and 8 TeV c.m.e.
- ⋆ 2011 7 TeV and then 2012 8 TeV datasets (will) allow for precise measurements of W,Z physics properties and the determination of multiple differential cross-sections

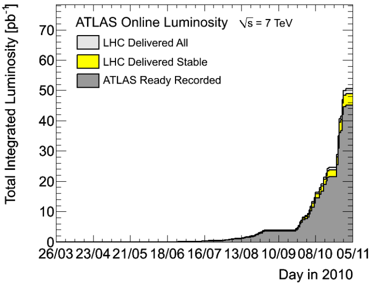

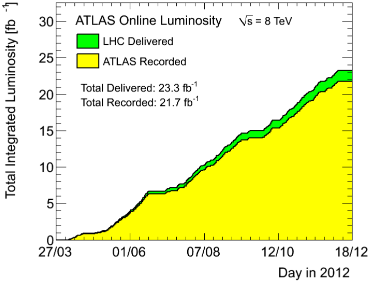

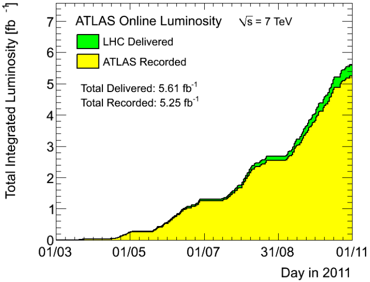

$W \to \ell\nu$ selection

- Single lepton triggers with high efficiency
- $p_{T,l} > 20$ GeV
  $|\eta_e| < 2.47$, $|\eta_\mu| < 2.4$
  (elec. excl. calo crack)
  isolated leptons
  $E_T^{\rm miss} > 25$ GeV
  $m_T > 40$ GeV
- QCD from data fitting E_T^{miss} (e) and studying control regions in $iso - E_T^{miss}$ plane (μ)
- $131 - 140\,K$ candidates with $7 - 9\,\%$ background

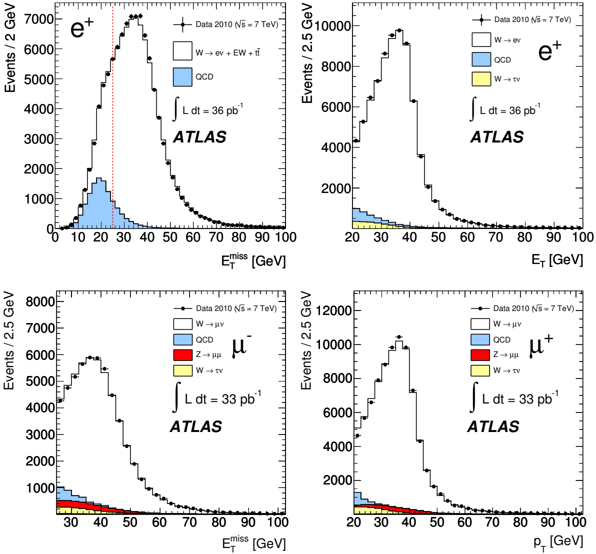

$Z \to \ell\ell$ selection

- ⋆ Single lepton triggers with high efficiency
- ⋆ $p_{T,l} > 20\ GeV$
  $|\eta_e| < 2.47$, $|\eta_\mu| < 2.4$
  (elec. excl. calo crack)
  isolated leptons
  opposite charge
  $66 < m_{\ell,\ell} < 116\ GeV$
- ⋆ QCD from data fitting $m_{\ell,\ell}$ lineshape and studying control regions in $(iso, m_{\ell,\ell})$
- ⋆ $\sim 10 - 12\,K$ candidates with $1 - 2\,\%$ background

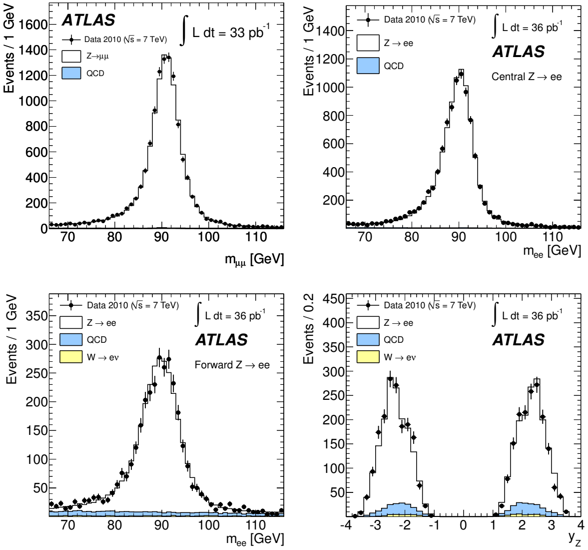

Precision of W and Z cross-sections with $\mathcal{L} = 35\, pb^{-1}$

- ⋆ $\delta\sigma_{W\to e\nu}$ of 1.8 – 2.0 %, dominated by electron reconstruction, identification and $E_{\mathrm{T}}^{\mathrm{miss}}$
- ⋆ $\delta\sigma_{Z\to ee}$ of 2.7 %, dominated by el. reconstruction and identification

- ⋆ $\delta\sigma_{W\to\mu\nu}$ of 1.6 – 1.7 %, dominated by muon efficiencies, QCD background and $E_{\mathrm{T}}^{\mathrm{miss}}$
- ⋆ $\delta\sigma_{Z\to\mu\mu}$ of 0.9 %, dominated by muon efficiencies

Electron channels (%)	$W^{\pm}$	W^{+}	W^{-}	Z
Trigger	0.4	0.4	0.4	<0.1
Electron reconstruction	0.8	0.8	0.8	1.6
Electron identification	0.9	0.8	1.1	1.8
Electron isolation	0.3	0.3	0.3	—
Electron energy scale and resol.	0.5	0.5	0.5	0.2
Non-operational LAr channels	0.4	0.4	0.4	0.8
Charge misidentification	0.0	0.1	0.1	0.6
QCD background	0.4	0.4	0.4	0.7
Electroweak+$t\bar{t}$ background	0.2	0.2	0.2	<0.1
E_T^{miss} scale and resolution	0.8	0.7	1.0	—
Pile-up modeling	0.3	0.3	0.3	0.3
Vertex position	0.1	0.1	0.1	0.1
$C_{W/Z}$ theoretical uncertainty	0.6	0.6	0.6	0.3
Total experimental uncertainty	**1.8**	**1.8**	**2.0**	**2.7**
$A_{W/Z}$ theoretical uncertainty	1.5	1.7	2.0	2.0
Total excluding luminosity	2.3	2.4	2.8	3.3
Luminosity	3.4			

Muon channels (%)	$W^{\pm}$	W^{+}	W^{-}	Z
Trigger	0.5	0.5	0.5	0.1
Muon reconstruction	0.3	0.3	0.3	0.6
Muon isolation	0.2	0.2	0.2	0.3
Muon p_{T} resolution	0.04	0.03	0.05	0.02
Muon p_{T} scale	0.4	0.6	0.6	0.2
QCD background	0.6	0.5	0.8	0.3
Electroweak+$t\bar{t}$ background	0.4	0.3	0.4	0.02
E_T^{miss} resolution and scale	0.5	0.4	0.6	-
Pile-up modeling	0.3	0.3	0.3	0.3
Vertex position	0.1	0.1	0.1	0.1
$C_{W/Z}$ theoretical uncertainty	0.8	0.8	0.7	0.3
Total experimental uncertainty	**1.6**	**1.7**	**1.7**	**0.9**
$A_{W/Z}$ theoretical uncertainty	1.5	1.6	2.1	2.0
Total excluding luminosity	2.1	2.3	2.6	2.2
Luminosity	3.4			

W and Z cross-sections with $\mathcal{L} = 35\,pb^{-1}$ vs. Theory

- ⋆ Comparing in the fiducial region disentangles theor. and exp. effects
- ⋆ This enables more interesting comparisons among different PDF sets
- ⋆ First dedicated calculation of NNLO predictions based on FEWZ and DYNNLO with experimental cuts

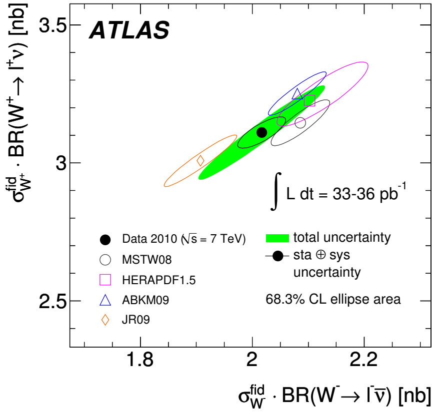

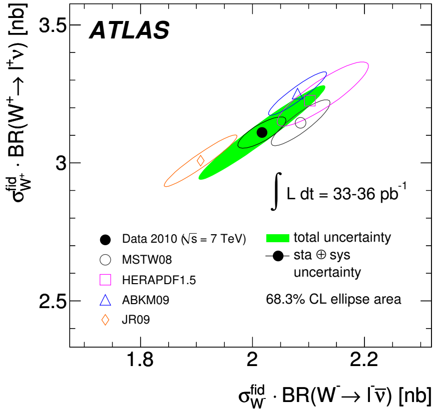

W and Z cross-sections with $\mathcal{L} = 35\,pb^{-1}$ vs. Theory /2

- ⋆ $W^{\pm}/Z$, W^{+}/W^{-} ratios profit from exp. and theor. systematics cancellation
- ⋆ $W^{\pm}/Z$ ratio measured with total uncert. of 1.5 %, W^{+}/W^{-} with 1.7 %

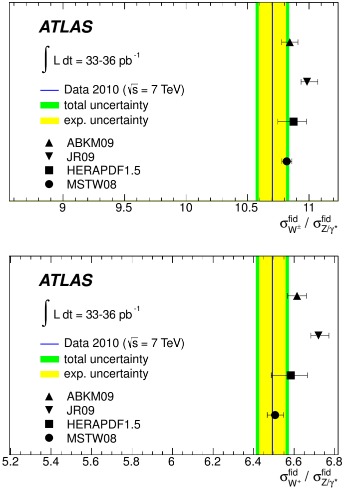

W and Z cross-sections with $\mathcal{L} = 35\,pb^{-1}$ vs. Theory /3

★ New measurements of the ratios of the e and μ branching fractions

$$R_W = \frac{\sigma_W^e}{\sigma_W^\mu} = \frac{Br(W \to e\nu)}{Br(W \to \mu\nu)} = 1.006 \pm 0.004\,(\text{sta}) \pm 0.006\,(\text{unc}) \pm 0.023\,(\text{cor}) = 1.006 \pm 0.024$$

$$R_Z = \frac{\sigma_Z^e}{\sigma_Z^\mu} = \frac{Br(Z \to ee)}{Br(Z \to \mu\mu)} = 1.018 \pm 0.014\,(\text{sta}) \pm 0.016\,(\text{unc}) \pm 0.028\,(\text{cor}) = 1.018 \pm 0.031$$

★ Inserting R_Z PDG value into the present measurement for a combined cross section analysis

⇒ reduction of correlated R_W systematic uncertainty

⇒ improved result of $R_W = 0.999 \pm 0.021$.

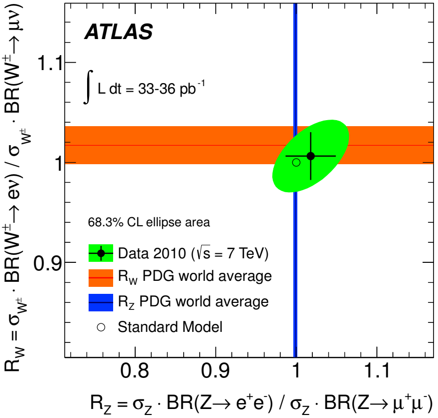

W and Z cross-sections with $\mathcal{L} = 35\,pb^{-1}$ vs. Theory /4

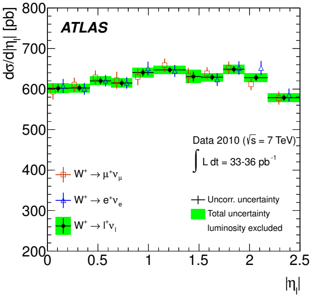

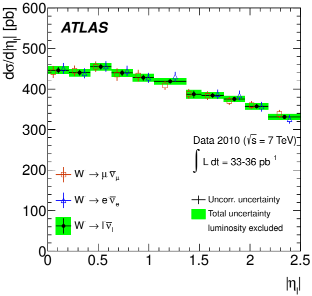

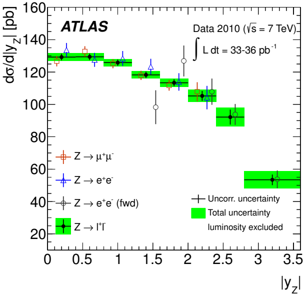

- ★ e and μ measurements combined **with full covariance matrix available** ($\chi^2/ndf = 33.9/29$)
- ★ Z rapidity coverage up to $|y| = 3.5$ including the forward $Z \to ee$
- ★ Accuracy ~ **2 % for $|y_Z| < 2$ and W**, ~ 6 (10) % at $|y_Z| = 2.6\,(3.2)$

W and Z cross-sections with $\mathcal{L} = 35\,pb^{-1}$ vs. Theory /4

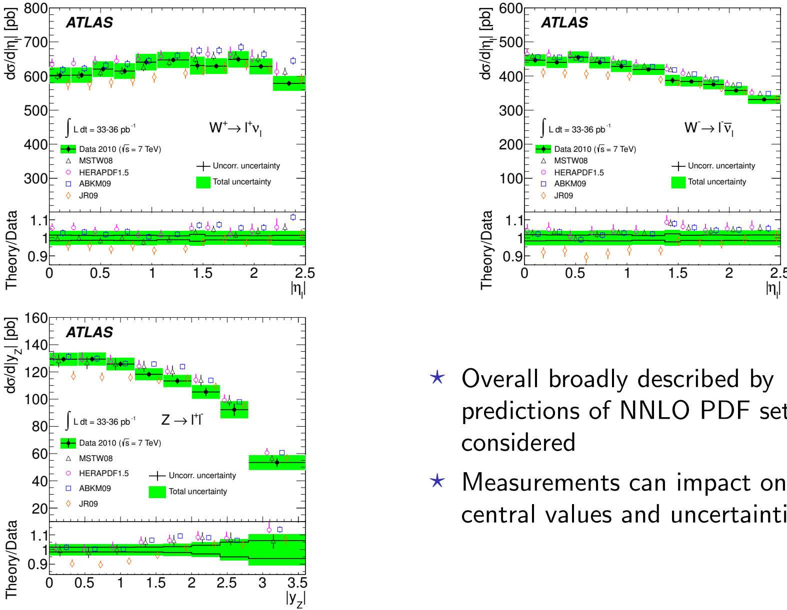

- ⋆ Overall broadly described by predictions of NNLO PDF sets considered
- ⋆ Measurements can impact on PDF central values and uncertainties ...

QCD analysis of W and Z data with $\mathcal{L} = 35\, pb^{-1}$

- ⋆ Little is known about light sea-quark separation at low x and, in particular, about the strange quark distribution, $s(x)$
  - ✓ Flavor SU(3) symmetry suggests equal light sea-quark distributions
  - ✓ However, the strange quarks may be suppressed due to their larger mass

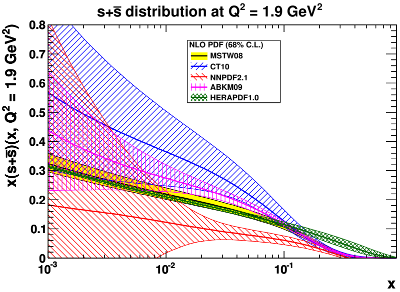

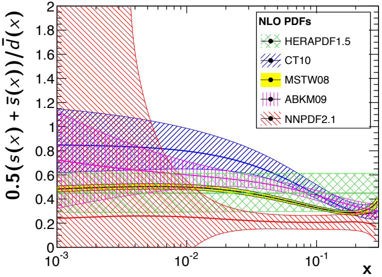

- ⋆ $s(x)$, $\bar{s}(x)$ accessed in CC ν-scattering $(W^+ s \rightarrow c,\ W^- \bar{s} \rightarrow \bar{c})$ at x ~ 0.1 and $Q^2 \sim 10$ GeV^2 by the NuTeV and CCFR experiments
  - ✓ Uncertainties from charm fragmentation and nuclear corrections
  - ✓ Results are compatible with either suppressed and unsuppressed strangeness

QCD analysis of W and Z data with $\mathcal{L} = 35\,pb^{-1}$

- ⋆ Little is known about light sea-quark separation at low x and, in particular, about the strange quark distribution, $s(x)$
  - ✓ Flavor SU(3) symmetry suggests equal light sea-quark distributions
  - ✓ However, the strange quarks may be suppressed due to their larger mass
- ⋆ Recent HERMES kaon multiplicity data point to a strong x dependence of $s(x)$ and rather large value of $x(s+\bar{s})$ at $x \sim 0.04$ and Q^2 1.3 GeV^2

Data interpretation depends on the knowledge of the fragmentation of strange quarks to K mesons at low Q^2

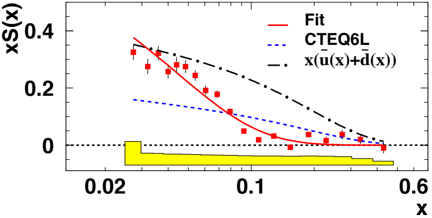

- ⋆ Nucleon strange density plays an important role in a wide range of physics
  - ✓ From measurements at p-p colliders of $W + c$ production and m_W to formation of strange matter and neutrino interactions at ultrahigh energies

QCD analysis of W and Z data with $\mathcal{L} = 35\,pb^{-1}$

- ⋆ HERA and ATLAS W,Z data is fit with the HERAFITTER framework with Q_0^2 1.9 GeV^2, m_c 1.4 GeV, m_b 4.75 GeV, $\alpha_s(M_Z)$ 0.1176
- ⋆ Fits are run with fixed $\bar{s}/\bar{d} = 0.5$ and leaving $\bar{s}(x)$ free (with $s = \bar{s}$)
- ⋆ The "free $\bar{s}$ fit" leads to better χ^2 to ATLAS data and determines

$$r_s = 0.5(s+\bar{s})/\bar{d} = \mathbf{1.00 \pm 0.20\,exp \pm 0.07\,mod^{+0.10}_{-0.15}\,par^{+0.06}_{-0.07}\,\alpha_S \pm 0.08\,th}$$

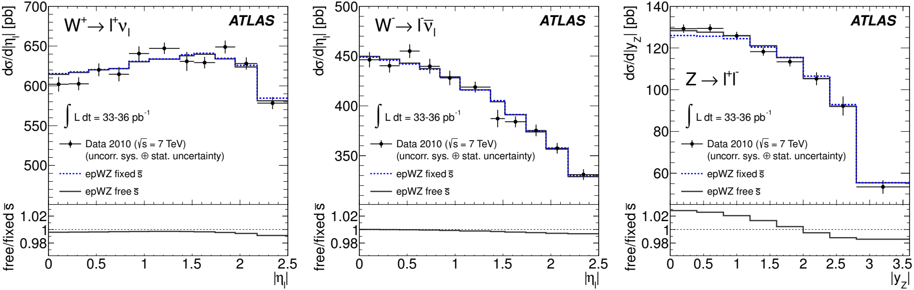

QCD analysis of W and Z data with $\mathcal{L} = 35\, pb^{-1}$

- ⋆ Fitted r_s value is compared to NNLO PDFs
- ⋆ Increase in strange leads to decrease in $\bar{u}, \bar{d}$ given the precise constrain given by F_2 HERA data at low x, total sea (Σ) increases by 8%
- ⋆ The prediction with "free $\bar{s}$ fit" leads to a better description of the measured W/Z ratio

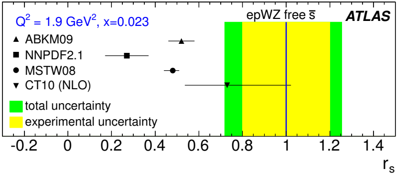

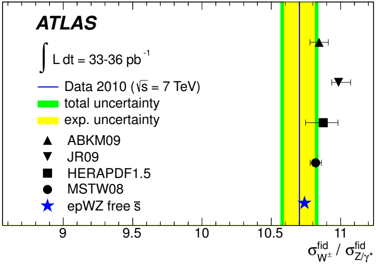

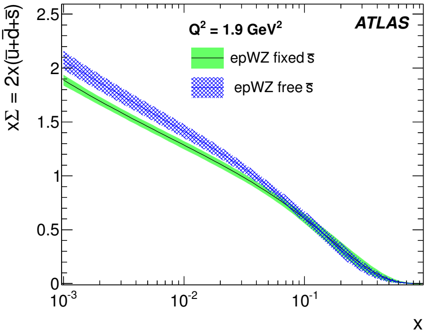

W+D cross-section measurement

- ⋆ Handle on strange quark PDF at $x \sim 0.01$ (eg. important for W mass)
  - ✓ SU(3) flavour, symmetric light quark sea? or due to strange mass, strange suppression? dependence on x? $s - \bar{s}$ asymmetry?

- ⋆ Exclusive reconstruction of four $D(^*)^+$ decay channels exploiting the lepton-D charge correlation: OS-SS subtraction ⇒ fit sig/bkg templates ⇒ unfold

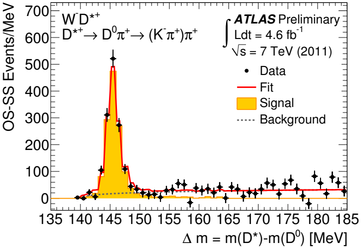

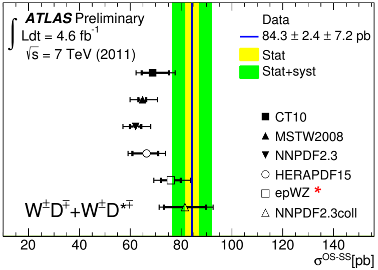

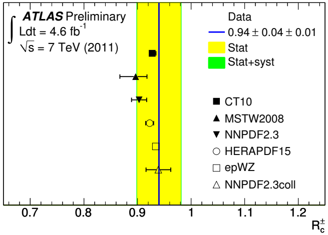

* epWZ = HERA+ATLAS W,Z 2010 PDF

Boson p_T measurements in $W \to \ell\nu$ and $Z \to \ell\ell$ decays

- ⋆ Boson p_T in $Z \to \ell\ell$ decays

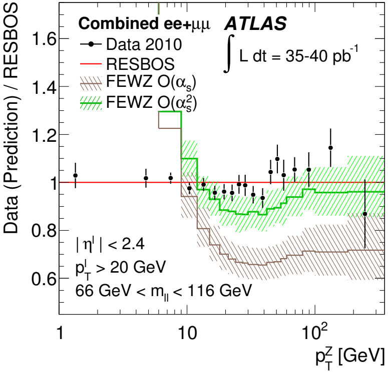

- ⋆ Boson p_T in $W \to \ell\nu$ decays

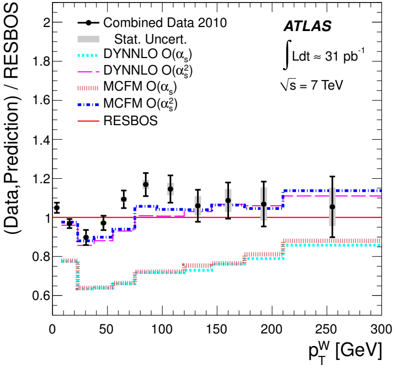

Boson p_T measurements in $W \to \ell\nu$ and $Z \to \ell\ell$ decays

★ Uncertainties

$\langle p_T^Z \rangle$ (GeV)	$\frac{1}{\sigma^{\text{fid}}}\frac{d\sigma^{\text{fid}}}{dp_T^Z}$ (GeV^{-1})	stat. (%)	syst. (%)	A_c^{-1}	unc. (%)
1.3	0.0366	2.0	4.7	1.047	3.7
4.8	0.0586	1.5	3.6	1.029	1.8
7.5	0.0466	1.7	1.5	1.014	1.5
10	0.0348	1.9	1.6	0.999	1.5
13	0.0277	2.2	1.7	0.999	1.4
16	0.0210	2.5	1.7	0.990	1.5
19	0.0167	2.8	1.8	0.989	1.5
22	0.0133	3.1	1.9	0.990	1.5
25	0.0112	3.4	2.0	0.994	2.3
28	0.0092	4.0	2.1	0.988	2.3
33	0.0067	3.2	2.1	0.987	3.2
39	0.0047	3.8	2.3	0.979	3.9
45	0.0038	4.2	2.4	0.965	4.3
51	0.0030	4.9	2.5	0.950	4.4
57	0.0021	5.7	2.7	0.938	5.3
69	0.0013	4.0	2.8	0.910	5.3
89	$5.5 \cdot 10^{-4}$	6.1	3.1	0.894	5.3
132	$1.6 \cdot 10^{-4}$	5.9	3.7	0.826	5.4
245	$9.8 \cdot 10^{-6}$	15.6	5.4	0.672	5.6

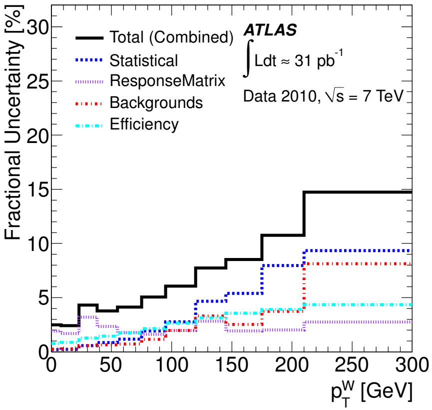

Boson p_T measurements in $W \to \ell\nu$ and $Z \to \ell\ell$ decays

★ Comparison of measurements with 2010 data

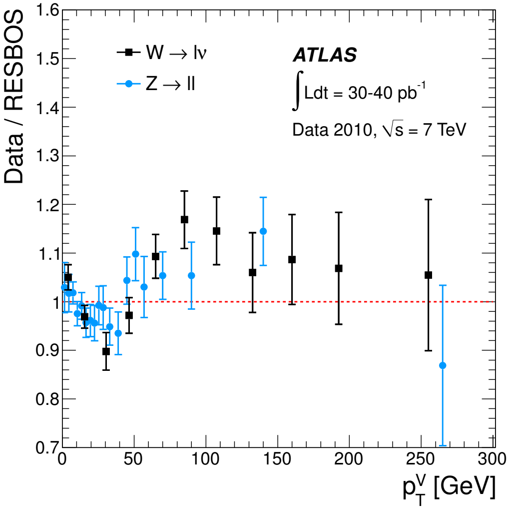

Z boson ϕ^* definition

- ⋆ Angular observable $\propto p_T^Z/m_{\ell\ell} \Rightarrow \phi^* \equiv tan(\phi_{acop}/2) \cdot sin(\theta^*_\eta)$ (defined in A. Banfi et al., Eur. Phys. J. C 71 (2011) 1600)
  - ✓ $\phi_{acop} \equiv \pi - \Delta\phi$, $\Delta\phi$ being the azimuthal opening angle between the two leptons
  - ✓ $cos(\theta^*_\eta) \equiv tanh[(\eta^- - \eta^+)/2]$ is a measure of the scattering angle of the leptons with respect to the proton beam direction in the rest frame of the dilepton system.

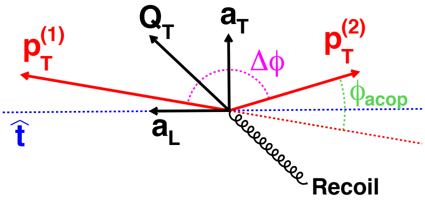

- ⋆ 99% of events have $\Delta\phi > \pi/2$
- ⋆ $\hat{t} = (p_T^1 - p_T^2)/|p_T^1 - p_T^2|$, p_T^i vector in plane transverse to beam direction
- ⋆ $\frac{\Delta(a_T/m_{\ell\ell})}{(a_T/m_{\ell\ell})} = \left(\frac{p_T^2}{p_T^1+p_T^2} - \frac{1}{2}\right)\frac{\Delta p_T^1}{p_T^1}$ The ratio is less sensitive to p_T uncertainties

$a_T/m_{\ell\ell} \approx tan(\phi_{acop}/2) sin(\theta^*)$, θ^* defined with a Lorentz boost along the beam direction such that the two leptons are back-to-back in $r-\theta$ plane. This boost corresponds to $\beta = tanh[(\eta^- + \eta^+)/2]$ yielding to $cos(\theta^*_\eta) = tanh[(\eta^- - \eta^+)/2]$

Z boson ϕ^* measurement

- ⋆ Correlation between ϕ^* and boson p_T

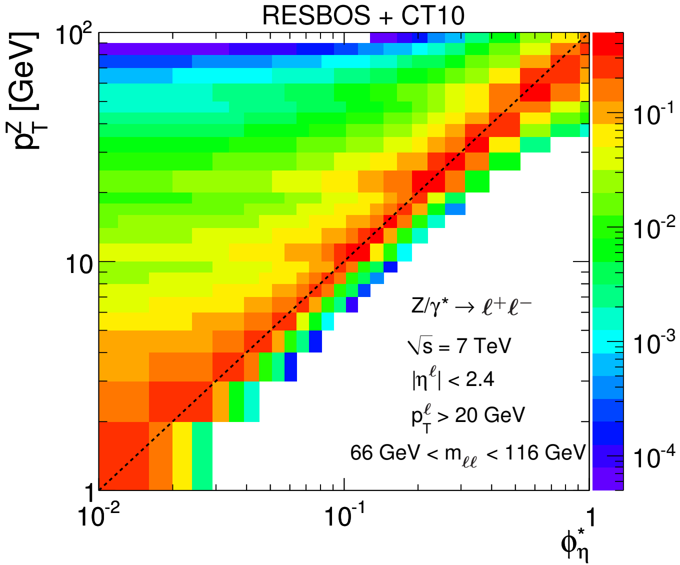

Z boson ϕ^* measurement

★ Comparison of ϕ^* measurement in $Z \to \ell\ell$ decays to Banfi et al. (NNLL-NLO) and FEWZ (NNLO)

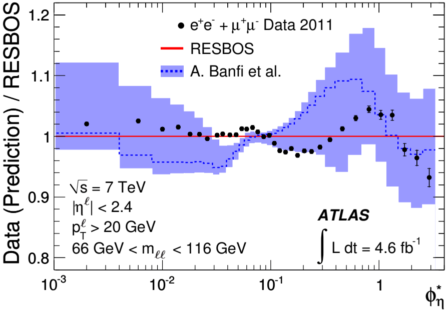

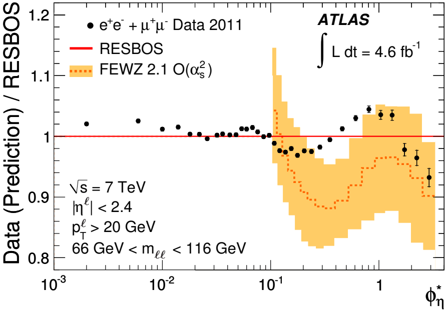

High mass Drell-Yan cross-sections

⋆ Cross-section at "dressed level" compared to MC predictions without (left) and with (right) QCD-EW K-factors

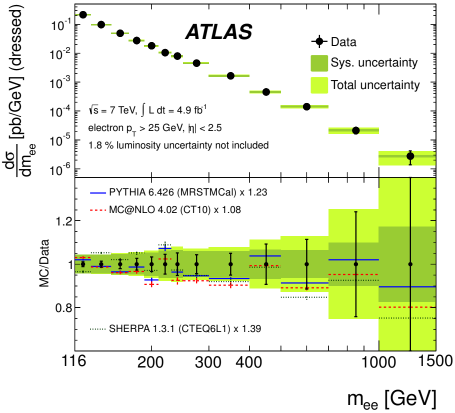

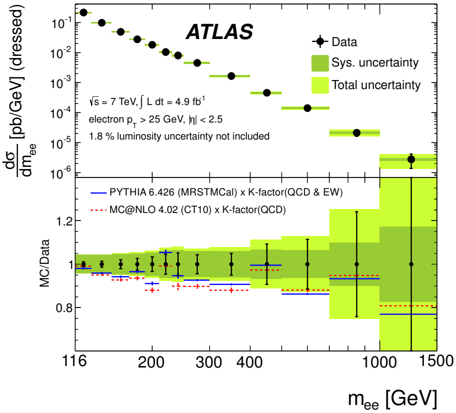

including FSR photons in a cone $\Delta R < 0.1$

High mass Drell-Yan cross-sections

- ⋆ Purity (fraction of reconstructed events generated in the same bin) as a function of m_{ee}

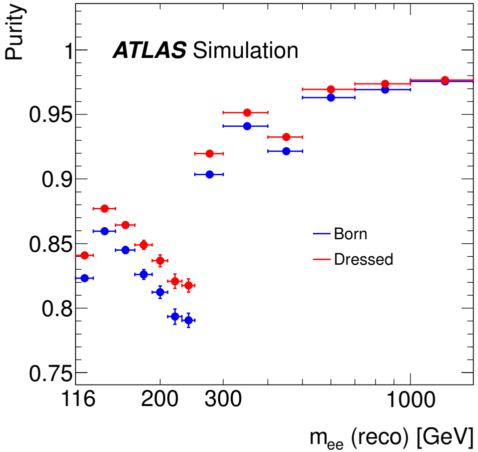

Forward-backward Z asymmetry measurement

★ Distributions of $cos\theta^*_{CS}$ for muons, central and forward electrons

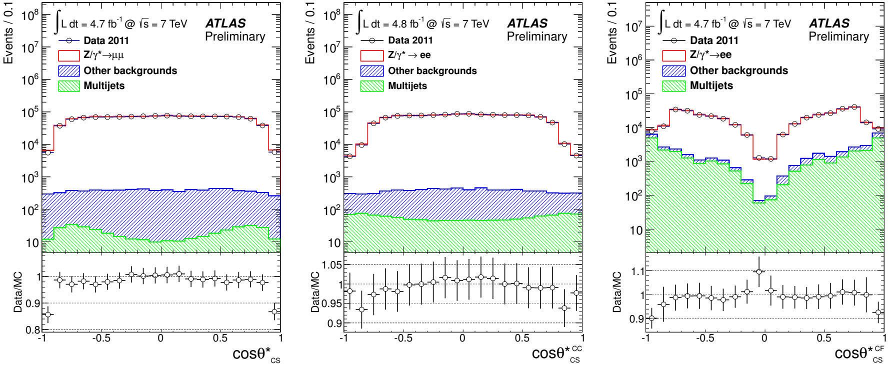

$$A_{FB} = \frac{N_{cos\theta^*_{CS}\geq 0} - N_{cos\theta^*_{CS}<0}}{N_{cos\theta^*_{CS}\geq 0} + N_{cos\theta^*_{CS}<0}} \quad , \quad cos\theta^*_{CS} = \frac{p_z(\ell^+\ell^-)}{|p_z(\ell^+\ell^-)|}\frac{2(p_1^+ p_2^- - p_1^- p_2^+)}{m(\ell^+\ell^-)\sqrt{m(\ell^+\ell^-)^2 + p_T(\ell^+\ell^-)^2}}$$

Forward-backward Z asymmetry measurement

- ⋆ Raw A_{FB} distributions for muons, central and forward electrons, after background subtraction (restricted in the region around the Z pole)

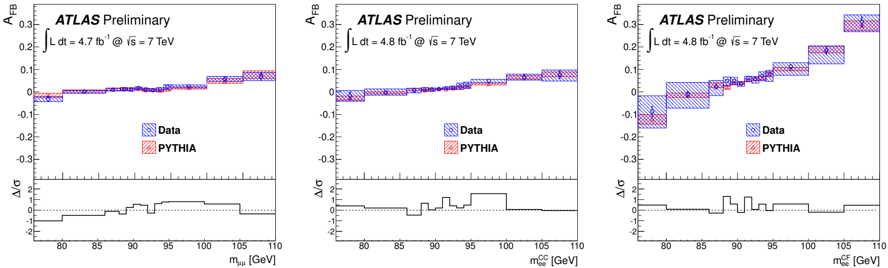

Forward-backward Z asymmetry measurement

★ Raw A_{FB} distributions for muons, central and forward electrons, after background subtraction

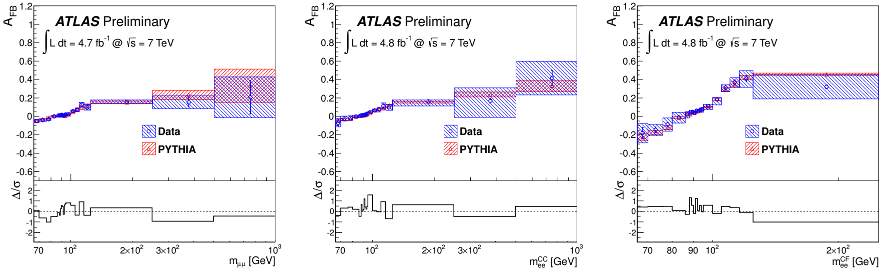

Forward-backward Z asymmetry measurement

⋆ Unfolded A_{FB} spectrum compared to PYTHIA prediction including QED FSR and NLO QCD corrections (not corrected also for dilution effect)

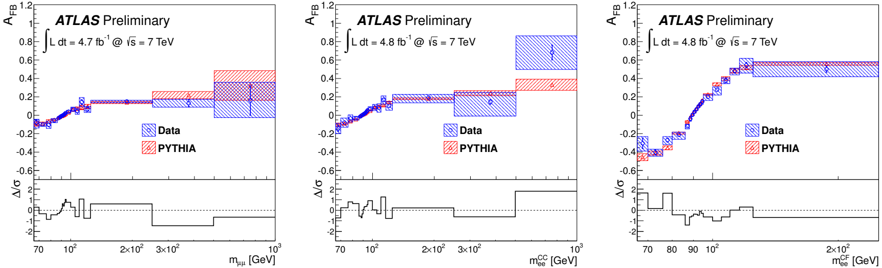

Forward-backward Z asymmetry measurement

⋆ Fully unfolded A_{FB} spectrum compared to PYTHIA prediction including QED FSR and NLO QCD corrections (corrected also for dilution effect)

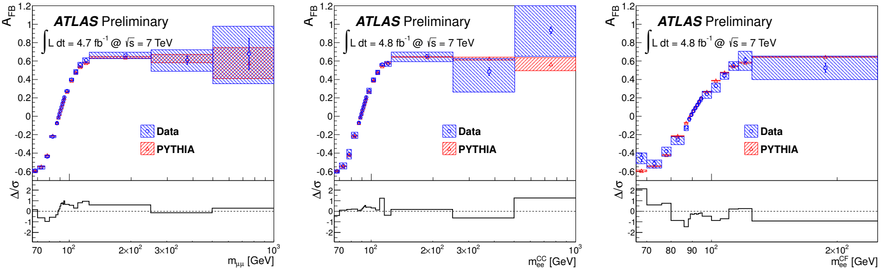

W polarization at high p_T

- ⋆ Cosine of the helicity angle of the lepton from W decay at generator-level
- ⋆ Solid lines are without selection, dashed lines are after all acceptance plus m_T^W cuts except the η_ℓ cuts and dotted lines are after all acceptance plus m_T^W cuts
- ⋆ "All events" distributions are normalised to unity

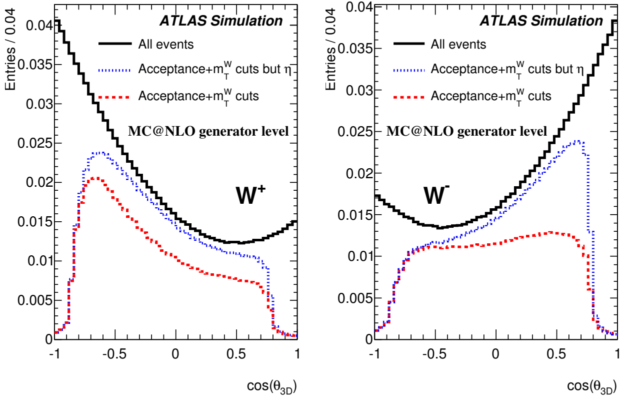

W polarization at high p_T

- Representation of $cos\theta_{2D}$ as a function of $cos\theta_{3D}$ in events where the W transverse momentum is greater than 50 GeV
- Events are simulated with MC@NLO after acceptance and m_T^W cuts

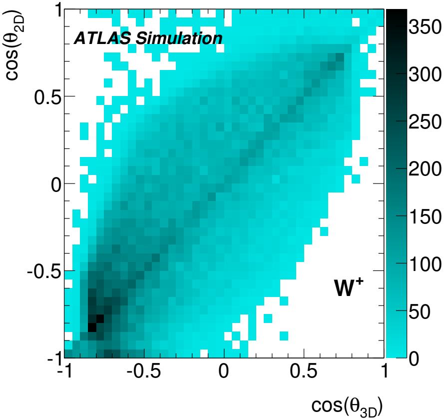

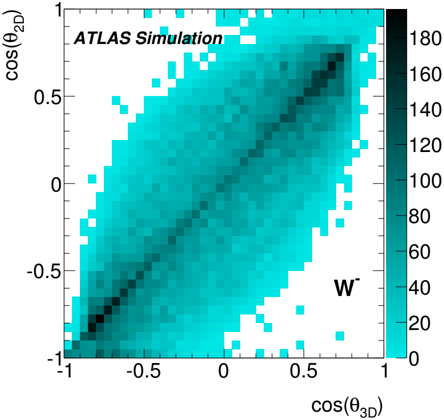

W polarization at high p_T

- Results of the fits to $cos\theta_{2D}$ distributions using helicity templates for $W \rightarrow \mu\nu$ events with $35 < p_T^W < 50\ GeV$, after background subtraction

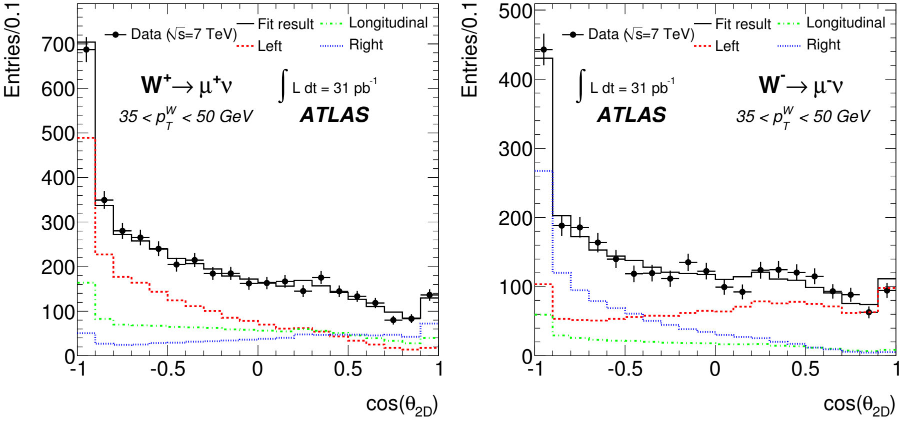

W polarization at high p_T

★ Results of the fits to $cos\theta_{2D}$ distributions using helicity templates for $W \to e\nu$ events with $35 < p_T^W < 50\ GeV$, after background subtraction

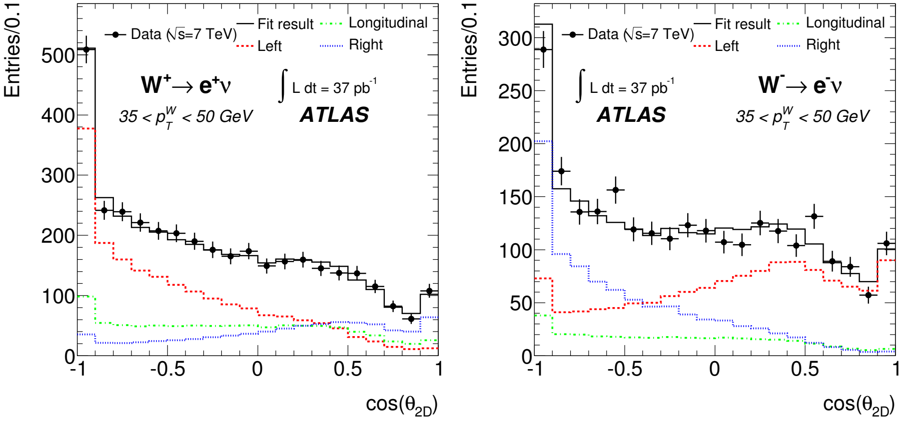

W polarization at high p_T

- ⋆ Results of the fits to $cos\theta_{2D}$ distributions using helicity templates for $W \to \mu\nu$ events with $p_T^W > 50\,GeV$, after background subtraction

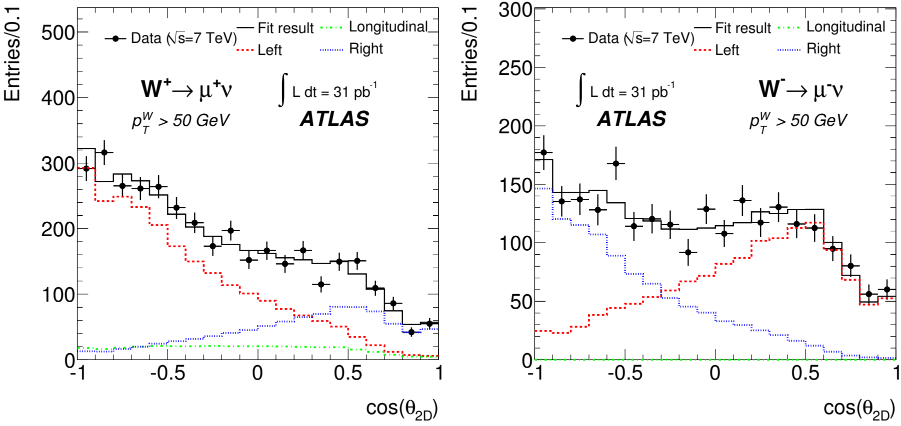

W polarization at high p_T

- ⋆ Results of the fits to $cos\theta_{2D}$ distributions using helicity templates for $W \to e\nu$ events with $p_T^W > 50\ GeV$, after background subtraction

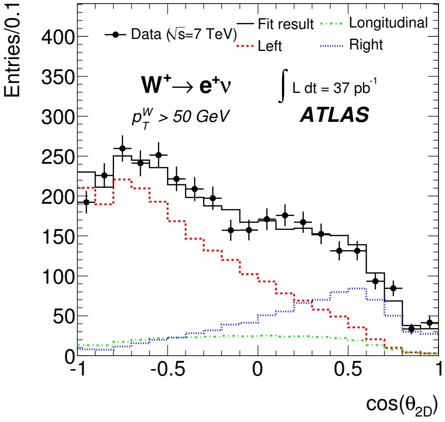

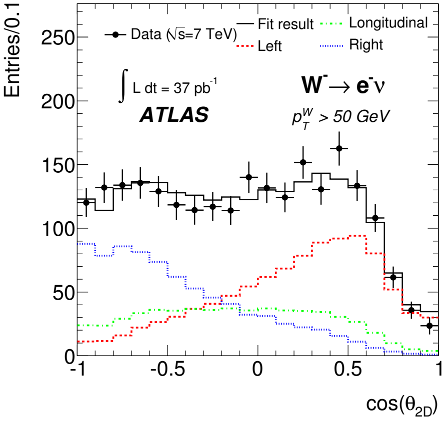

W polarization at high p_T

- ⋆ Measured values of f_0 and $f_L - f_R$ within acceptance cuts for $35 < p_T^W < 50\ GeV$ (left) and $p_T^W > 50\ GeV$ (right), compared to MC@NLO and POWHEG predictions